

## Molecular beam induced changes in adsorption behavior of NO on NiO(111)/Ni(111)

B. D. Zion<sup>a)</sup> and S. J. Sibener<sup>b)</sup>

*The James Franck Institute and Department of Chemistry, Gordon Center for Integrative Science, The University of Chicago, 929 East 57th Street, Chicago, Illinois 60637, USA*

(Received 18 September 2006; accepted 28 August 2007; published online 19 October 2007)

We have examined the adsorption behavior at  $\sim 110$  K of NO on NiO(111) overlayers prepared on a Ni(111) substrate. High-resolution electron-energy-loss spectroscopy shows fundamental changes in the vibrational spectrum for the beam dosed surface in comparison with the background dosed surface. Three vibrational peaks are observed after beam dosing, two of which are not observed after conventional background dosing. The peaks can be assigned to NO stretches for a previously observed NO state, a new NO bonding geometry, and a new NO<sub>2</sub> surface species, previously unobserved under NO dosing. The difference is accounted for by increased NO uptake due both to kinetically activated adsorption and to increased exposure. © 2007 American Institute of Physics. [DOI: 10.1063/1.2786987]

### INTRODUCTION

Nickel, like other commonly used metals, forms a naturally self-passivating, thin multilayer oxide surface as the natural saturation point for the oxidation process. For this reason, it is among the most useful metals because the NiO barrier at the surface protects the bulk from further reaction with oxygen. Under ambient atmospheric conditions surface reactions will take place on this NiO surface rather than the underlying bulk metal. These reactions will pertain to the use of nickel as machine parts, in airframes or catalytic devices. Understanding reactions at the NiO surface is fundamental in understanding the usefulness of this metal in real world applications.

The present article will focus on the interaction of adsorbates on a fully grown thin layer of nickel oxide on the metal substrate. We show that molecular beam dosing of NiO/Ni with NO leads to the creation of a novel overlayer. Monitoring the surface with high-resolution electron-energy-loss spectroscopy (HREELS), we see two new vibrational peaks in addition to a previously identified surface N–O stretch. We assign one of the novel vibrational features to a new, bent NO surface species by comparison to organometallic NO ligands and the other to a molecular NO<sub>2</sub> formed on the surface similar to the vibrational spectrum of NO<sub>2</sub> dosed NiO.

The NiO surface exhibits complex behavior with respect to basic questions of surface chemistry. It is well-known that different surfaces of a metal often have highly different behaviors, such as reactivities and work functions. These differences are largely due to the density of surface atoms and the arrangement of atoms leading to corrugations, kinks, and

steps. When we consider a rock salt structure such as NiO, the picture becomes further complicated by the presence of two atomic species.

Experimental studies have shown that two oxide surfaces are commonly formed in reaction of pure nickel with oxygen.<sup>1–9</sup> These surfaces are NiO(100) and NiO(111) which present rather different geometries. Either the (111) or (100) face of the Ni can be oxidized under O<sub>2</sub> exposure to form a thin film of either the (111) or (100) face of NiO, depending on oxidation conditions. The Ni(111) surface, used in this study, oxidizes to NiO(100) at elevated temperatures but forms NiO(111) when exposed to oxygen at room temperature, which persists after formation on annealing to 600 K. This latter preparation technique and surface are employed in the current study.

The focus of this work is on the interaction of NO with the oxide surface. There are some subtle differences in the adsorption behavior of NO on the different NiO(100) and NiO(111) surfaces, but the general behavior is very similar. Saturation coverage is achieved at approximately 12 L exposure. HREELS spectra of these systems show the NiO phonon structure with only one additional peak due to the NO stretching vibration in the 220–225 meV region, somewhat redshifted from the gas phase value of 232 meV.<sup>10–13</sup> Thermal desorption from this surface shows varied results depending on the surface and the study, but all show desorption at  $\sim 200$  K either broadly peaked or with nearby minor peaks.<sup>10,12,14–18</sup>

In all of these previous studies, the surface was dosed by backfilling the chamber with NO. In the present experiment, surface dosing was achieved by means of a molecular beam of NO. We might expect changes in surface behavior under beam dosing and certain differences as we significantly increase the dosing rate. However, as we will see, the new surface features monitored in these experiments cannot be explained simply by changes in surface dosing rate.

<sup>a)</sup>Present Address: Department of Chemistry, Pennsylvania State University, University Park, PA 16802.

<sup>b)</sup>Author to whom correspondence should be addressed. Electronic mail: s-sibener@uchicago.edu

## EXPERIMENTAL

The experiments were conducted in a two level ultrahigh vacuum scattering chamber with a connected molecular beamline. The ultimate pressure of the chamber is less than  $1 \times 10^{-10}$  Torr. The chamber is equipped with a HREEL spectrometer, model LK2000, a molecular beamline, a temperature controlled sample mount, and various surface preparation and characterization apparatuses. A detailed description of the machine can be found in a previous publication.<sup>19</sup>

The sample used for the present work is a nickel single crystal, cut and polished to within  $0.2^\circ$  of the close-packed (111) plane. The Ni sample is cleaned by repeated cycles of argon ion sputtering at a backing pressure of  $5 \times 10^{-5}$  Torr and annealing at 1100 K until Auger electron spectroscopy (AES) shows a clean surface. The clean sample has a very sharp low-energy electron diffraction (LEED) pattern with six-fold symmetry. Further treatment of the clean surface to prepare a NiO(111) surface is done by exposing the sample to  $1 \times 10^{-7}$  Torr of  $O_2$  for 15 min to an hour followed by annealing to 600 K for 10 min. The thin oxide surface exhibits diffuse LEED spots with sixfold symmetry with spots slightly closer together in reciprocal space than the clean Ni(111) due to the relatively larger lattice constant in real space. The AES shows oxygen and nickel signals that are nearly equal in peak-to-peak height. This surface is retreated between experiments by annealing to 600 K for 10 min. The NO adsorption work was conducted on this preparation of the surface.

The prepared substrate was cooled to a base temperature of 110 K before NO exposure. The dosing beam was weakly supersonic and had a mean kinetic energy of  $\sim 75$  meV with a full width at half maximum resolution of  $\sim 60$  meV. For some measurements, NO dosing was accomplished by backfilling the main chamber to a certain pressure of ambient NO gas. In all cases, HREELS data were taken to monitor the surface species present.

## RESULTS

Figure 1 shows HREEL spectra of NiO after various exposures by backfill to NO, which is the experimental method used by previous researchers. The clean NiO shows the phonon at  $\sim 70$  meV and a series of NiO phonon overtones of decreasing intensity at multiples of  $\sim 70$  meV. After 16 L NO dosing, the HREELS shows an additional peak at 225 meV in agreement with previous vibrational studies of the NO reaction with NiO. Between 16 and 25 L NO exposures, the spectra do not change significantly, indicating that a saturation point has been reached. This picture had been the most commonly held understanding of the interaction of NO with this surface. However, at extended exposure, two additional peaks, one at 160 meV and the other at 197 meV, become clearly visible and the initial peak at 225 meV shifts to 230 meV. The emergence of these new vibrational signatures requires approximately an order of magnitude longer exposure to the background NO.

Figure 2 shows a series of HREEL spectra of the surface after incremental NO molecular beam dosing. As in the case of the backfill spectra, the 225 meV peak emerges initially,

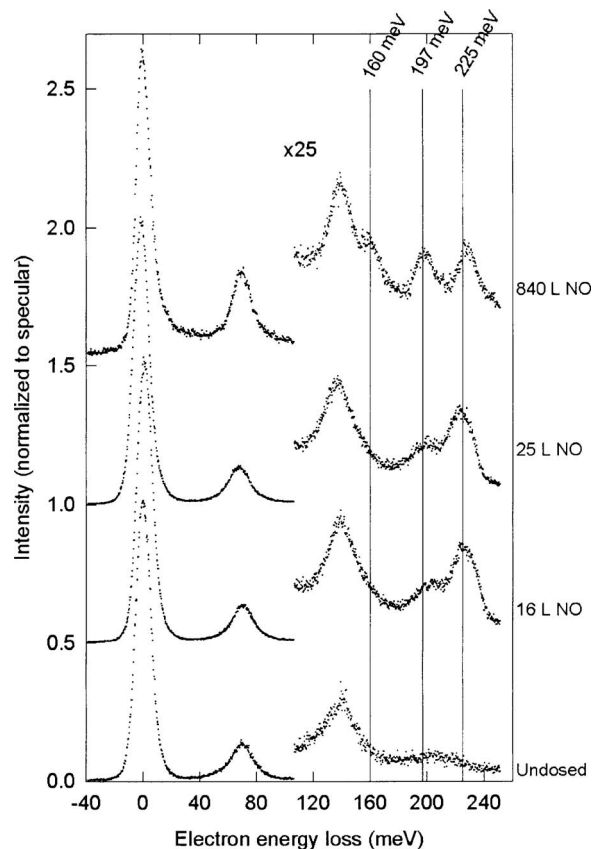


FIG. 1. HREEL spectra of NiO, both clean and NO dosed. The bottom spectrum is clean NiO where the NiO phonon and the first and second overtones are recognizable. The next three spectra are from overlayers produced by backfilling with NO. The vibrational spectrum does not change significantly between 16 and 25 L, agreeing with the notion of saturation after  $\sim 12$  L NO exposure. However, extended dosing shows the growth of additional peaks.

followed by the shift to 230 meV and the appearance of the two additional vibrational peaks after which all the peaks increase in intensity throughout the exposure. There is a great similarity between the spectra recorded at 3, 4, and 5 min of beam exposure (corresponding to 38, 51, and 64 L, respectively) and the 840 L backfill dose, indicating that the beam dosed surface reaches a certain coverage at approximately an order of magnitude less total exposure to NO as the backfill-dosed surface. Clearly, the use of the molecular beam accelerates the surface reaction process with NO. Figure 3 shows the difference spectra between the dosed and undosed surface data presented in Fig. 2 in the region of 125–250 meV electron-energy loss. The subtraction of the clean NiO surface spectrum accounts for the phonon features and allows us to see the emergence of the NO overlayer vibrational features. Between 6.4 and 12.7 L beam exposures, the 160 meV feature begins to appear but at these low exposures, is difficult to quantify. In these figures, the elastic reflection, the NiO phonons at 70, 140, and 210 meV, as well as the three vibrational features of interest at 160, 197, and 230 meV have been fitted with Gaussian curves for purposes of normalization and integration. Figure 4 shows plots of the ratios of peak intensities to elastic scattering intensity for the 230, 197, 160 meV vibrational features. In these figures, we see a similar behavior for each of the three features, an initial

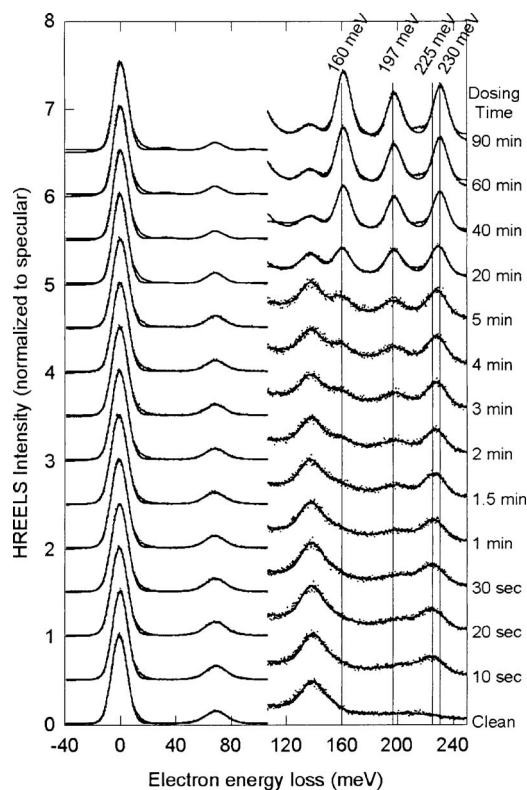


FIG. 2. Series of HREEL spectra taken after successive amounts of exposure to a pure NO beam. The exposure rate is 12.7 L/min. In the series, three distinct peaks grow in simultaneously near 160, 197, and 225 meV. The lines are a guide to the eye. The higher energy peak shifts in energy as it grows, from 225 to 230 meV. A small lower energy peak near 35 meV becomes visible at the higher exposures.

rapid uptake to a certain intensity followed by a long monotonic increase with further exposure to final saturation after  $\sim 1000$  L. The vibrational peaks at 230 and 197 meV are closely associated with the NO internal stretching vibration. However, the 160 meV vibrational peak is not representative of a known NO vibration but rather falls within the range indicative of  $\text{NO}_2$  or  $\text{N}_2\text{O}$  stretching motion.<sup>20–22</sup> The gas phase vibrational energy for the symmetric stretch of  $\text{NO}_2$  is 163.9 meV and for the N–O stretch of the  $\text{N}_2\text{O}$  is 159.3 meV.<sup>23</sup>

Figure 5 shows a series of HREEL spectra of the 110 K NiO surface dosed with  $\text{NO}_2$ . After a few minutes of  $\text{NO}_2$  dosing, clear peaks centered around 160 and 215 meV become visible. Unfortunately, as dosing continues longer than approximately 10 min, all of the energy-loss signals attenuate even while the elastic reflectance increases. The result is that no surface vibrations are measured to any significant degree after 40 min.

## DISCUSSION

From the extended backfill dosing data in Fig. 1 it is clear that the plateau reached after  $\sim 16$  L of NO dosing is not the saturation point but merely some change in adsorption regime. Although dosing by ambient gas can achieve an extended surface coverage, beam directed dosing increases the rate of NO uptake. We have examined the stability of the vibrational signals after beam dosing at 110 and 125 K. At

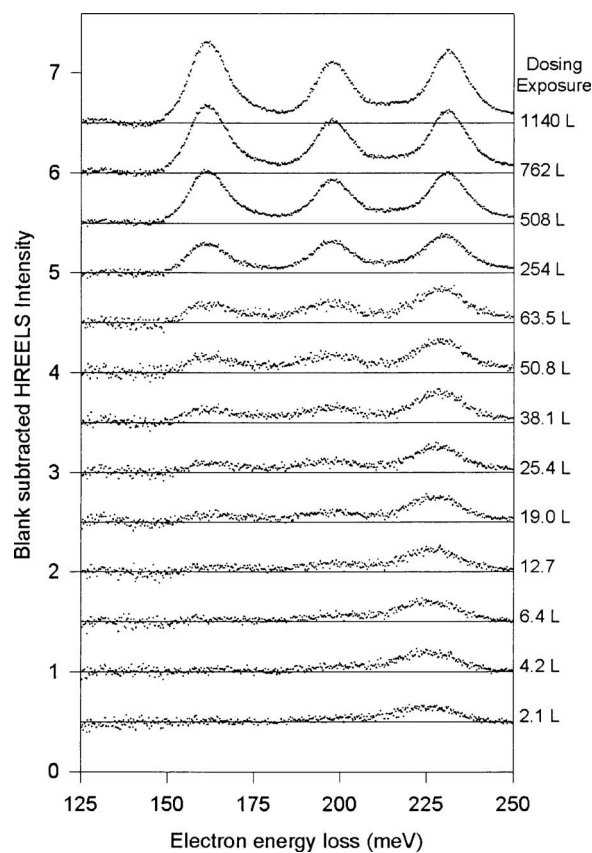


FIG. 3. Blank subtracted HREEL spectra. These are the same data presented in Fig. 2 showing only the region of interest. The spectrum of the undosed surface adjusted by a normalization factor has been subtracted from each data set in order to remove the NiO phonon signal, leaving only the spectra due to the NO adsorbate. This method of data analysis shows the difficulty in assigning an intensity for the loss features at low NO exposure, especially for features located near substrate vibrational features.

110 K we see an initial attenuation in the two lower energy vibrations during the first several hours until a steady state is achieved. When a similarly 110 K doses NO surface layer is heated to 125 K for a fixed time and subsequently recooled to 110 K to collect HREEL spectra, we see that only 5 min of annealing is required to achieve a spectrum identical to that of the steady state at 110 K. It may be that the lowest temperature used in this study of 110 K is on the cusp of an additional stable binding site. Another possibility is that by dosing with a higher intensity in the form of a molecular beam, the effective surface pressure pushes us into a regime of high coverage on the Langmuir isotherm. Once the beam is turned off, the effective pressure drops to zero and desorption eventually attenuates the vibrational signal to the steady state level. This view is also supported by the fact that the increase in vibrational signal is more dependent on the dosing rate than on total exposure. Nonetheless, the steady state observed in these experiments has not been previously observed.

The preparation detailed above provides a NiO(111)/Ni(111) surface, but because the lattice constants for NiO and Ni cubic cells are 4.19 and 3.52 Å, respectively,<sup>9</sup> which give rise to a lattice mismatch of 19%, a highly defective surface is expected. On such a surface, experimental determination of the reconstruction is difficult,

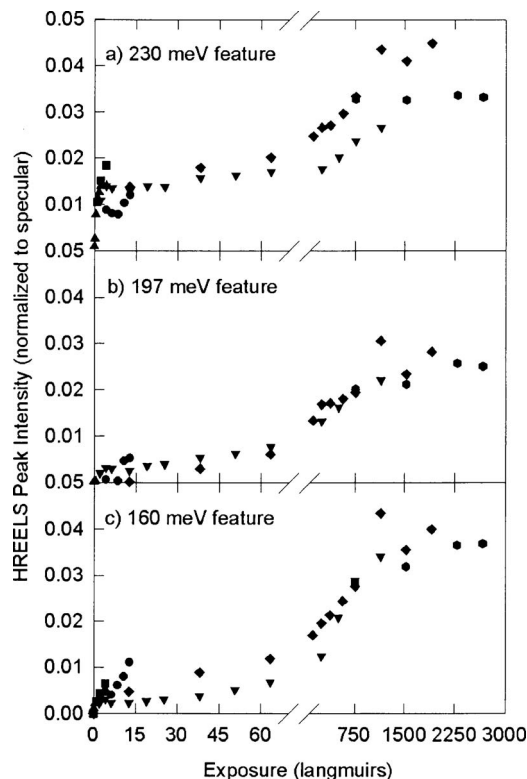


FIG. 4. Peak intensity ratio of the individual loss features to elastic signal as a function of beam dosing exposure. The data points are obtained from the peak fits of the various vibrational features in Fig. 2. Panels (a), (b), and (c) show the ratios for the 230, 197, and 160 meV features, respectively. The different symbols represent different data sets.

and, therefore, the extent of octopolar reconstruction and hydroxyl coverage was not directly measured. The peak shift of the highest energy NO vibration seen in Fig. 2 can be explained in terms of dehydroxylation of the surface. In previous experiments,<sup>13</sup> a 5 meV blueshift in NO vibrational frequency was seen between the hydroxylated and the dehydroxylated NiO(111).

From HREELS measurements taken after annealing to various temperatures and from data in Fig. 4, it is seen that during adsorption and thermal desorption, the relative intensity of the three peaks remains constant. The absence of independent adsorption or thermal desorption behavior of any of these vibrational signals beyond the initial plateau is indicative of a single adsorption site on the surface. We would expect different uptake curves and different desorption temperatures if these vibrational signals were due to different adsorption sites.

The two higher vibrational frequencies lie within a range indicative of NO stretching, whereas the lower lying peak can be associated with  $N_2O$  or  $NO_2$  stretching motion. We conducted experiments dosing with a  $N_2O$  beam and found absolutely no sticking on the surface. We therefore eliminate this molecule as a possible explanation of the vibrational peak. Data obtained via  $NO_2$  dosing (Fig. 5) give a partial explanation of the origin of the 160 meV vibrational peak. We imagine two channels for  $NO_2$  adsorption, one being a dissociative mechanism which selectively results in only the 215 meV peak and the second being intact  $NO_2$  adsorption giving rise to the 160 meV peak. These results are similar to

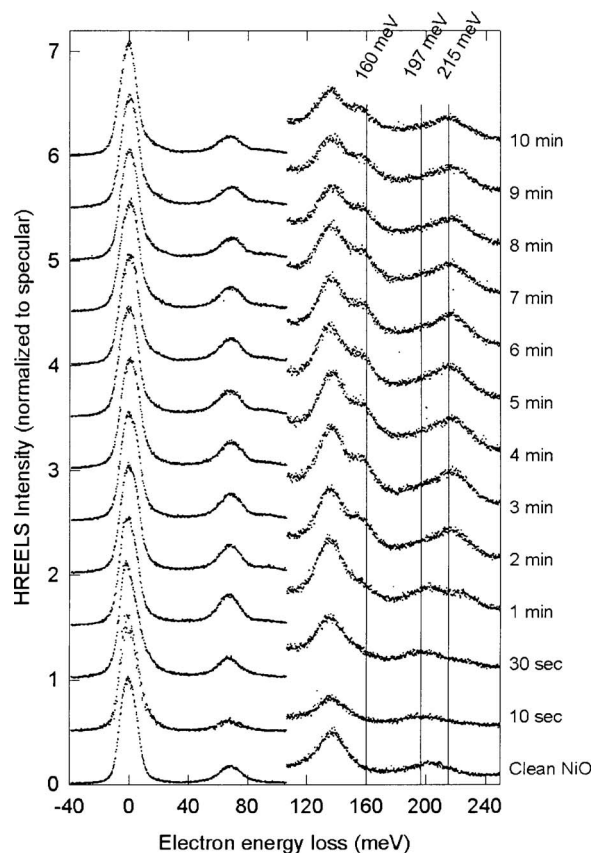


FIG. 5. Series of HREEL spectra of the 110 K substrate taken after successive amounts of exposure to a pure  $NO_2$  beam. In the series, two peaks grow in simultaneously near 160 and 215 meV. These two peaks are observed in Fig. 2 for the NO dosed surface. Absent is the central 197 meV peak. The vibrational spectra attenuate with extended dosing.

those shown in Fig. 2 with the notable absence of the 197 meV peak. It is not clear why the dissociation would result in only one of the probable NO vibrational frequencies, nor is it clear that the 160 meV peak must be due to intact nascent  $NO_2$ .

$NO$  stretching frequencies have been observed at 197 meV on bare Ni(111) (Ref. 24) and on NiO at 225 meV. The nitrite vibrational frequencies of the free ion are 165 and 156 meV for the symmetric and asymmetric stretching modes, respectively, and a bending energy at 102 meV.<sup>20</sup> In several organometallic compounds, a chelating  $NO_2$  has been observed to have vibrations in the ranges of 158–161 meV assigned to the symmetric stretch, 148–150 meV assigned to the asymmetric stretch, and 107 meV assigned to the bending mode.<sup>21</sup> We are led to believe that the behavior observed upon NO beam dosing is caused by a rapid adsorption of NO as previously determined by other researchers, but then a surface reaction occurs with the impinging NO molecules after saturation, the incoming molecules forming some  $NO_2$  on the NiO. Because the new peaks are not readily formed under ambient dosing conditions, we believe that the higher dosant concentration at the surface increases the reaction rate dramatically, thus requiring a fraction of the total dose to achieve the same results as in a backfill experiment. From our data we see that the increase in vibrational signal after NO dosing is more dependent on the dosing rate than the

total exposure. In addition, because the NO uptake rate is invariant with dosing angle, the normal energy component of the incident energy is not the determining factor in adsorption. This rules out a normal energy scaling mechanism that would have strongly preferred the directed dose of a molecular beam technique.

One result from this work is the emergence of two new vibrational peaks in the NO/NiO system under molecular beam dosing conditions not seen in previous backfill experiments. The vibrational frequency for the new lower energy peak at 160 meV lies between the free nitrite ion asymmetric and symmetric stretching frequencies at 156 and 165 meV, respectively. The nitro bonding geometry, which has the nitrogen atom bonded to the surface, is known in organometallic chemistry to have higher vibrational frequencies for both stretches. For this bonding geometry to be present in our study, we would be observing the asymmetric stretch and not the symmetric stretch. Therefore, this bonding geometry is unlikely because the asymmetric stretch in this geometry is not dipole active and thus not detectable by HREELS. The nitro bonding geometry notwithstanding, there are five nitrito bonding geometries where the oxygen is bound directly to the surface. Of these geometries, only the chelating structure with both oxygens bound to a surface atom allows for the symmetric stretch to be uniquely observed. The organometallic data show that the vibrational frequencies of the chelated NO<sub>2</sub> are not significantly shifted from the free nitrite. Because of the resolution of the spectrometer, it would not be possible to resolve two peaks separated by less than 10 meV, and also, the shifts in vibrational energy of NO<sub>2</sub> on the NiO surface may not be the same as in other organometallic systems. Therefore, other surface orientations cannot be ruled out as possible binding geometries.<sup>20</sup>

The other newly detected vibrational peak at 197 meV has two possible origins. The 197 meV frequency is the vibrational energy measured by HREELS for NO on clean Ni(111).<sup>24</sup> Incomplete oxidation or some kind of surface reduction of patches back to nickel could account for the observation of a vibration at this energy. However, this explanation is highly implausible due to the increase in all three principle vibrational peaks with exposure. If patches of bare nickel were being formed on which NO was adsorbing, we would expect a concurrent decrease in vibrational signal from species adsorbed on the NiO surface. A better model is based on the idea that NO adsorbed to a surface acts in two basic ways, a three electron donor NO<sup>+</sup> linear species or a one electron donor NO<sup>-</sup> bent species.<sup>20</sup> Figure 6(a) shows the two bonding geometries with their measured vibrational energies. In one organometallic compound, [RuCl(NO)<sub>2</sub>(P(C<sub>6</sub>H<sub>5</sub>)<sub>3</sub>)<sub>2</sub>]<sup>+</sup>, where the two NO ligands are bound in each of the geometries, the measured vibrational energies are 229 and 208 meV for the linear and bent species, respectively.<sup>25</sup> Figure 6(b) shows this ruthenium complex depicting the two different NO bonding geometries and indicating their vibrational energies. Therefore, the peak at 230 meV can be assigned to the linear bonding geometry and the 197 meV peak is believed to be the bent form of the NO adsorbate.

The HREEL spectra reveal more details of the effects of

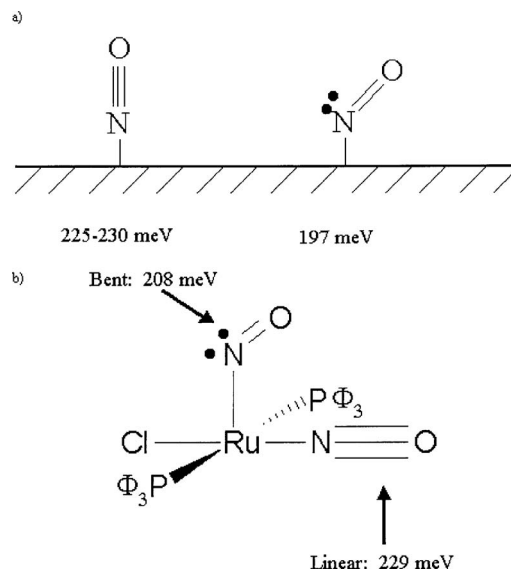


FIG. 6. (a) Schematic representation of the proposed bonding geometries. The species on the left, bound normal to the surface, represents the NO<sup>+</sup>, one electron donor, and the species on the right is the “bent,” NO<sup>-</sup>, three electron donor. (b) Molecular configuration of [RuCl(NO)<sub>2</sub>(P(C<sub>6</sub>H<sub>5</sub>)<sub>3</sub>)<sub>2</sub>]<sup>+</sup>. The vibrational frequencies of both the linear and bent NO ligands are given (Ref. 23).

molecular beam dosing of NO on the NiO surface. From recent experiments of NO adsorbed on vacuum cleaved NiO(100), multilayer NO ice desorption occurs at 56 K and no further desorption signal is observed until 145 K where a small peak is measured. The main submultilayer desorption peaks are measured at 216 and 220 K. Likewise for NO adsorbed on the NiO(100) thin film grown on Ni(100), only the tail end of a broad 145 K desorption peak is observed in the temperature region below 200 K.<sup>26</sup> In our case, HREELS data taken after sequential annealings to various temperatures show attenuation below 140 K of the majority of the intensities of the three vibrational peaks resultant from NO beam dosing. The 197 meV peak drops quickly with temperature and has completely dissipated by 140 K. The 160 meV peak is slightly more durable, retaining some intensity until 160 K, although it is difficult to be sure that this signal is not due to the closely lying NiO phonon at 140 meV. Use of the identical curve fitting routines on spectra for the clean NiO before dosing and the depleted surface after annealing to 160 K shows a persistence of the 160 meV peak. The 230 meV peak, which is the conventionally observed vibration, maintains a significant signal similar in intensity to that produced in the early stages of beam dosing and by backfill dosing. We believe that the NO<sub>2</sub> and NO<sup>-</sup> surface species are eliminated by the rise in temperature to 140–160 K range. Although the 160 and 197 meV peaks desorb in a very similar temperature range, these two species are not necessarily related.

## SUMMARY

We have used a molecular beam of NO to dose thin layer NiO(111) grown on a Ni(111) substrate. The vibrational signature, which is monitored by *in situ* HREELS, changes dramatically for the NO beam dosed overlayer compared to NiO

surfaces dosed with NO by ambient gas dosing. In addition to observing a much greater intensity for the previously observed vibrational peak at 230 meV, two previously unobserved vibrations are seen in this system. By analogy to organometallic NO ligands, we assign the higher-lying frequency at 197 meV to a bent bonding geometry for NO. The lower energy peak is comparable to the HREEL spectrum for NiO dosed with a NO<sub>2</sub> beam and is therefore assigned to a stretching vibration from molecular NO<sub>2</sub> formed in a reaction on the surface.

## ACKNOWLEDGMENTS

This work was primarily supported by the Chemical Sciences, Geosciences and Biosciences Division, Office of Basic Energy Sciences, Office of Science, U.S. Department of Energy under Grant No. DE-FG02-00ER15089. We also acknowledge support from the AFOSR and infrastructure support from the NSF-Materials Research Science and Engineering Center at the University of Chicago under Grant No. NSF-DMR-0213745.

<sup>1</sup>V. E. Henrich and P. A. Cox, *The Surface Science of Metal Oxides* (Cambridge University Press, Cambridge, 1994).

<sup>2</sup>O. L. Warren and P. A. Thiel, *J. Chem. Phys.* **100**, 659 (1994).

<sup>3</sup>F. Rohr, K. Wirth, J. Libuda, D. Cappus, M. Bäumer, and H.-J. Freund, *Surf. Sci.* **315**, L977 (1994).

<sup>4</sup>N. Kitakatsu, V. Maurice, and P. Marcus, *Surf. Sci.* **411**, 215 (1998).

<sup>5</sup>N. Kitakatsu, V. Maurice, C. Hinnen, and P. Marcus, *Surf. Sci.* **407**, 36 (1998).

<sup>6</sup>A. Barbier, G. Renaud, C. Mocuta, and A. Stierle, *Surf. Sci.* **433–435**, 761 (1999).

<sup>7</sup>T. M. Christensen, C. Raoul, and J. M. Blakely, *Appl. Surf. Sci.* **26**, 408 (1986).

<sup>8</sup>W.-D. Wang, N. J. Wu, and P. A. Thiel, *J. Chem. Phys.* **92**, 2025 (1990).

<sup>9</sup>C. A. Ventrice and H. Geisler, in *Thin Films: Heteroepitaxial Systems*, edited by A. W. K. Liu and M. B. Santos (World Scientific, Singapore, 1999), pp. 167–209.

<sup>10</sup>H. Kuhlenbeck, G. Odörfer, R. Jaeger, G. Illing, M. Menges, T. Mull, H.-J. Freund, M. Pöhlchen, V. Staemmler, S. Witzel, C. Scharfschwerdt, K. Wennemann, T. Liedtke, and M. Neumann, *Phys. Rev. B* **43**, 1969 (1991).

<sup>11</sup>H. Kuhlenbeck, *Appl. Phys. A: Solids Surf.* **59**, 469 (1994).

<sup>12</sup>T. Mull, M. Menges, B. Baumeister, G. Odörfer, H. Geisler, G. Illing, R. M. Jaeger, H. Kuhlenbeck, H.-J. Freund, D. Weide, U. Schüller, P. Andersen, F. Budde, P. Ferm, V. Hamza, and G. Ertl, *Phys. Scr.* **41**, 134 (1990).

<sup>13</sup>M. Schönnenbeck, D. Cappus, J. Klinkmann, H.-J. Freund, L. G. M. Pettersen, and P. S. Bagus, *Surf. Sci.* **347**, 337 (1996).

<sup>14</sup>D. Cappus, C. Xu, D. Ehrlich, B. Dillmann, C. A. Ventrice, K. Al-Shamery, H. Kuhlenbeck, and H.-J. Freund, *Chem. Phys.* **177**, 533 (1993).

<sup>15</sup>M. Bäumer, D. Cappus, G. Illing, H. Kuhlenbeck, and H.-J. Freund, *J. Vac. Sci. Technol. A* **10**, 2407 (1992).

<sup>16</sup>H. Kuhlenbeck, G. Odörfer, R. Jaeger, C. Xu, T. Mull, B. Baumeister, G. Illing, M. Menges, H.-J. Freund, D. Weide, P. Andersen, G. Watson, and E. W. Plummer, *Vacuum* **41**, 34 (1990).

<sup>17</sup>J. Yoshinobu, X. Guo, and J. T. Yates Jr., *J. Chem. Phys.* **92**, 7700 (1990).

<sup>18</sup>J. Yoshinobu, X. Guo, and J. T. Yates Jr., *J. Vac. Sci. Technol. A* **9**, 1726 (1991).

<sup>19</sup>B. D. Zion, A. T. Hanbicki, and S. J. Sibener, *Surf. Sci.* **417**, L1154 (1998).

<sup>20</sup>M. R. Albert and J. T. Yates, *The Surface Scientist's Guide to Organometallic Chemistry* (American Chemical Society, Washington, D.C., 1987).

<sup>21</sup>D. M. L. Goodgame and M. A. Hitchman, *Inorg. Chem.* **4**, 721 (1965).

<sup>22</sup>C. Panja and B. E. Koel, *J. Phys. Chem. A* **104**, 2486 (2000).

<sup>23</sup>F. Mélen and M. Herman, *J. Phys. Chem. Ref. Data* **21**, 831 (1992).

<sup>24</sup>M. J. Stirniman, W. Li, and S. J. Sibener, *J. Chem. Phys.* **102**, 4699 (1995).

<sup>25</sup>C. G. Pierpont, D. G. V. Derveer, W. Durland, and R. Eisenberg, *J. Am. Chem. Soc.* **92**, 4760 (1970).

<sup>26</sup>R. Wichtendahl, M. Rodriguez-Rodrigo, U. Härtel, H. Kuhlenbeck, and H.-J. Freund, *Surf. Sci.* **423**, 90 (1999).